land

MDPI

Article

How to Achieve the Ecological Sustainability Goal of Ecologically Fragile Areas on the Qinghai-Tibet Plateau: A Multi-Scenario Simulation of Lanzhou-Xining Urban Agglomerations

Zeyuan Gong [1], Wei Liu [2], Jing Guo [3], Yi Su [1], Yapei Gao [1], Wanru Bu [4], Jun Ren [1,4,5,*] and Chengying Li [1,*]

[1] School of Civil Engineering, Qinghai University, Xining 810016, China; 19828020114@qhu.edu.cn (Z.G.); 200828020115@qhu.edu.cn (Y.S.); gaoyp@qhu.edu.cn (Y.G.)
[2] Qinghai Provincial Meteorological Service Center, Xining 810008, China; 202211050003@nuist.edu.cn
[3] Institute of Eco-Environment, Qinghai Academy of Social Sciences, Xining 810099, China; guojing@nwipb.cas.cn
[4] School of Finance and Economics, Qinghai University, Xining 810016, China; ys230951370772@qhu.edu.cn
[5] Graduate School, Qinghai University, Xining 810016, China
* Correspondence: renjun@qhu.edu.cn (J.R.); lichengying@qhu.edu.cn (C.L.)

Abstract: The future of the ecologically fragile areas on the Qinghai-Tibet Plateau (QTP) is a matter of concern. With the implementation of the Western Development Strategy, the Lanzhou-Xining Urban Agglomeration (LXUA) has encountered conflicts and compromises between urban expansion, ecological protection, and farmland protection policies in the rapid development of the past 2 decades. These deeply affect the land use layout, making the ecological sustainable development of the ecologically fragile areas of the QTP a complex and urgent issue. Exploring the impact of different policy-led land use patterns on regional ecosystem services is of great significance for the sustainable development of ecologically fragile areas and the formulation of relevant policies. Following the logical main line of "history-present-future", the Patch-level Land Use Simulation (PLUS) model, which explores potential factors of historical land use, and the Integrated Valuation of Ecosystem Services and Trade-offs (InVEST) model were used to construct three future scenarios for the modernization stage in 2031 dominated by different land use policies in this study. These scenarios include the Business-as-Usual Scenario (BS), the Cropland Protection Scenario (CP), and the Ecological Protection Scenario (EP). The study analyzed and predicted land use changes in the LXUA from 2001 to 2031 and assessed carbon storage, habitat quality at different time points, and water yield in 2021. The results indicated that land use changes from 2001 to 2021 reflect the impacts and conflicts among the Western Development Strategy, ecological protection policies, and cropland preservation policies. In 2031, construction land continues to increase under all three scenarios, expanding northwards around Lanzhou, consistent with the actual "northward expansion" trend of Lanzhou City. Changes in other land uses are in line with the directions guided by land use policy. By 2031, carbon storage and habitat quality decline under all scenarios, with the highest values observed in the EP scenario, the lowest carbon storage in the BS scenario, and the lowest habitat quality in the CP scenario. Regarding water yield, the LXUA primarily relies on alpine snowmelt, with construction land overlapping high evapotranspiration areas. Based on the assessment of ecosystem services, urban expansion, delineation of ecological red lines, and improvement of cropland quality in the LXUA were proposed. These findings and recommendations can provide a scientific basis for policy makers and planning managers in the future.

Keywords: urban agglomeration; ecosystem services; multi-scenario prediction; InVEST model; Lanzhou-Xining Urban Agglomeration

Citation: Gong, Z.; Liu, W.; Guo, J.; Su, Y.; Gao, Y.; Bu, W.; Ren, J.; Li, C. How to Achieve the Ecological Sustainability Goal of Ecologically Fragile Areas on the Qinghai-Tibet Plateau: A Multi-Scenario Simulation of Lanzhou-Xining Urban Agglomerations. *Land* **2024**, *13*, 1730. https://doi.org/10.3390/land13111730

Academic Editor: Jane Southworth

Received: 22 August 2024
Revised: 16 October 2024
Accepted: 19 October 2024
Published: 22 October 2024

1. Introduction

The Qinghai-Tibet Plateau (QTP), one of the most ecologically fragile areas in the world, is characterized by high altitude, cold temperatures, low precipitation, simple ecosystem structure, and weak resistance to disturbances [1]. The Lanzhou-Xining Urban Agglomeration (LXUA) is the only urban agglomeration designated by the Chinese government to be located in the ecologically fragile area of the Qinghai-Tibet Plateau. In the past 2 decades of development, the trajectory of the LXUA has reflected the urban development challenges faced by many cities in western China, profoundly affecting the regional land use structure and has made the ecological sustainable development of the ecologically fragile areas of the Qinghai-Tibet Plateau a complex issue. Conflicts and negotiations among urban expansion, ecological protection, and cropland preservation have been persistent issues throughout the growth of urban agglomeration. In 2001, the Chinese government initiated the Western Development Strategy, which included increasing investment in infrastructure construction in regions such as Qinghai Province and Gansu Province through central financial transfers and guidance to promote urbanization and resource development. According to the Western Development Strategy, the plan was divided into three phases: laying the foundation (2001), accelerating development (2011), and achieving modernization (2031) [2]. However, the actual implementation proved to be more complex than anticipated. The aggressive urban construction and development process led to an overemphasis on industrialization and an over-reliance on fixed asset investment and foreign investment. These factors continuously stimulated urban expansion demands and regional urban cooperation while posing potential threats to regional ecological security [3].

To address these issues, the government implemented a series of top-down environmental measures, such as the Natural Forest Protection Program and the Grain for Green Program, aimed at improving the harsh local ecological environment. These ecological measures achieved significant results [4]. However, with urban expansion, a large amount of high-quality cropland was encroached upon despite the cultivated land balance policy implemented by the central government in 1997. Studies have shown that urban expansion often converts high-productivity cropland into construction land while compensating with lower-productivity cropland in remote areas [5]. Additionally, the Chinese government initiated the Sloping Land Conversion Program (SLCP) in 1999, which demonstrated a tendency to sacrifice sloping cropland to restore ecosystems by reducing cropland area by 10% to gain more forest land [6]. This program was first piloted in Gansu Province and emphasized key implementation in western regions. The displacement of cropland by ecological projects exacerbated regional food security issues [7], prompting the Chinese government to further strengthen cropland preservation requirements during urban construction. The focus of cropland preservation is to maintain the dynamic balance of total cropland and emphasize the zoning and quality of basic farmland [8]. Currently, the Chinese government is enforcing strict delineation of ecological red lines in the Territorial Spatial Planning, which to some extent influences the layout of urban and rural construction land and urban morphology, thereby affecting the land use pattern of the LXUA.

Ecosystem services are the various benefits that humans obtain from natural ecosystems, including provisioning, regulating, supporting, and cultural services [9]. Studies have shown that land use changes have profound impacts on the supply and quality of ecosystem services [10]. The implementation of urban expansion, cropland preservation, and ecological protection policies changes land use types and spatial patterns, thereby affecting the level of ecosystem services in the region [11]. Ecosystem services not only reflect the health of ecosystems but also directly relate to regional sustainable development, especially in QTP ecologically fragile areas [12]. Therefore, exploring the impact of different policy-oriented land use patterns on ecosystem services in the LXUA and proposing balanced recommendations to meet QTP ecologically fragile area ecological sustainable development is of great significance.

Traditional Ecosystem Service Value (ESV) algorithms typically assess the overall value of ecosystem services based on economic indicators, which tends to overlook the spatial distribution and functional differences of specific ecosystem services [13]. In recent years, the integration of ecosystem service assessment and future urban land use simulation has become a major research focus in geography, ecology, and land resource sciences [14]. This study aims to construct multi-scenario simulation models to evaluate land use changes under different policy guidance in the LXUA and their impact on typical ecosystem services, as well as the spatial characteristics of these services. By combining the Patch-level Land Use Simulation (PLUS) model and the Integrated Valuation of Ecosystem Services and Trade-offs (InVEST) model, the study simulates land use changes under different policy scenarios and explores their impact on ecosystem services. The Land Expansion Analysis Strategy (LEAS) in the PLUS model can better uncover the drivers of historical land use changes [15], while the InVEST model's evaluation of different ecosystem services provides a multi-faceted perspective that includes quantitative analysis and spatial distribution [16]. Existing research on land use spatial pattern simulation and ecosystem service studies has focused on using coupled PLUS and InVEST models to study the impact and evolution of land use on single ecosystem services, with key areas including carbon storage [17], water yield [18], and habitat quality [19]. Additionally, if focusing solely on land use simulation, CA models have been widely applied and often coupled with various other models for research, including the Logistic model [20], Land Change Modeler (LCM) [21], and Markov model [22]. Addressing the contradictions in land use in the LXUA, previous studies focusing on predicting land use patterns and individual aspects of ecosystem services have been insufficient to propose comprehensive policy suggestions that account for different goals. This paper follows the "history-present-future" logical framework to simulate the land use change and provides an integrated assessment framework that comprehensively considers the impact of urban expansion, cropland preservation, and ecological protection on ecosystem services, and proposes coordinated suggestions to promote QTP ecologically fragile area ecological sustainable development. This study aims to provide scientific evidence for policymakers and planners through multi-scenario simulation and evaluation, striving to achieve a win-win situation for urban expansion, cropland preservation, and ecological protection.

2. Study Area and Data

2.1. Study Area

The LXUA includes all or part of the districts and counties of nine cities and prefectures in Gansu Province, including Lanzhou City, Baiyin City, Dingxi City, and Linxia Hui Autonomous Prefecture, as well as Xining City, Haidong City, Haibei Tibetan Autonomous Prefecture, Hainan Tibetan Autonomous Prefecture, and Huangnan Tibetan Autonomous Prefecture in Qinghai Province. The permanent population of the area is 11.93 million.

The data for the study area are based on the county-level administrative divisions announced by the Ministry of Civil Affairs of China as of 13 December 2022, extracting the above county-level administrative divisions to define the scope of the LXUA, as shown in Figure 1. The total area of the study area is 99,728.76 km^2. The LXUA is located in the transitional zone between the Qinghai-Tibet Plateau and the Loess Plateau, with the remnants of the Qilian Mountains in the north and the Huangshui Valley in the center. The region features a mix of mountains, hills, basins, and valleys, with an overall terrain that is high in the west and low in the east.

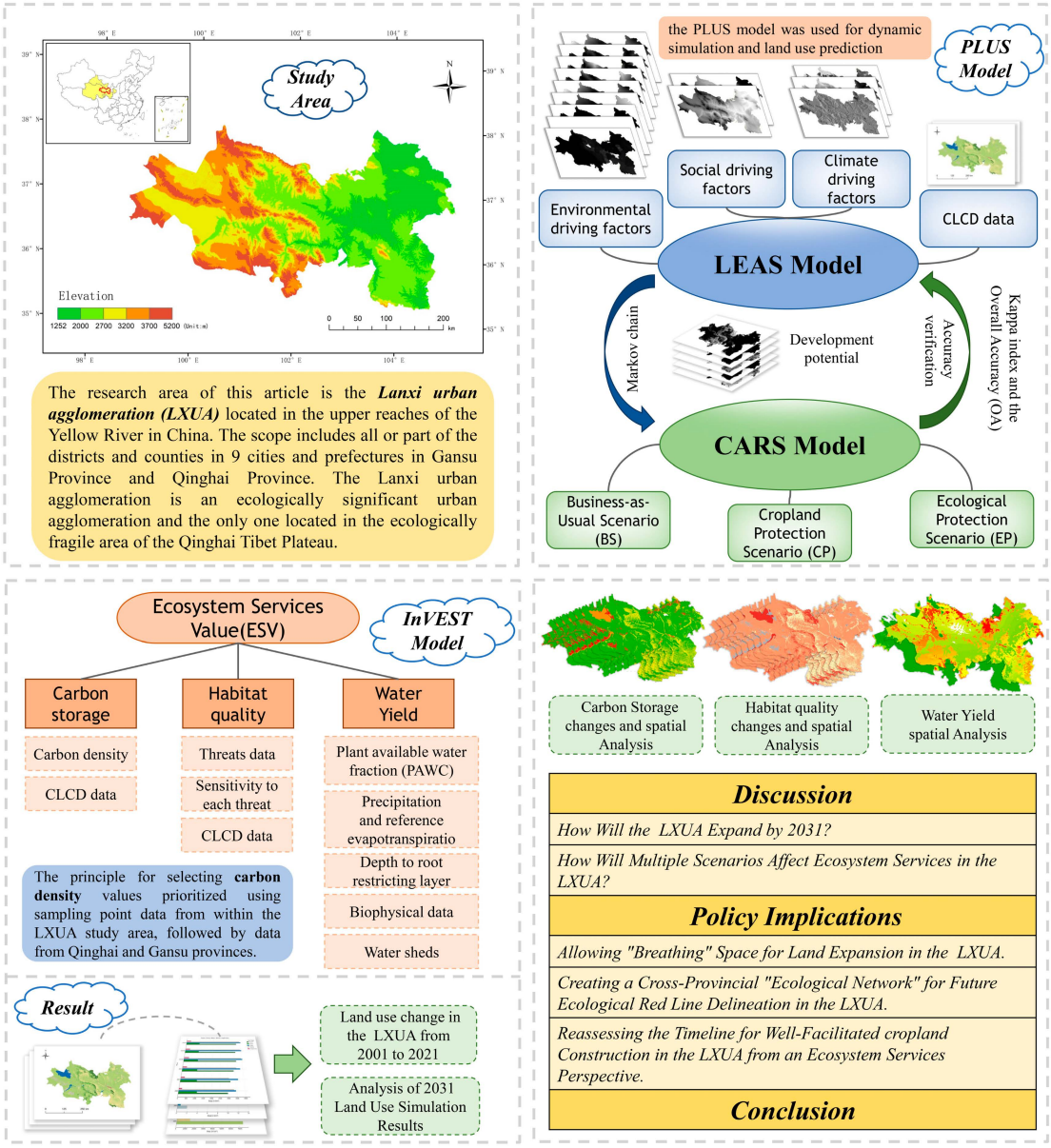

Figure 1. General research framework.

2.2. Data Sources and Processing

The CLCD data is derived from the 30 m CLCD dataset for China, released by Yang and Huang from Wuhan University in 2021 [23]. The overall accuracy of this CLCD dataset is 79.31%. Third party testing by the original authors showed that the CLCD's overall accuracy surpasses that of MCD12Q1, ESACCI_LC, FROM_GLC, and Globe Land 30. The classification system includes cropland, forest, shrubland, grassland, water, ice/snow, barren land, built-up land, and wetland. This system is similar to FROM_GLC and can be conveniently remapped to the Food and Agriculture Organization's system for subsequent InVEST model processing. Social factors in PLUS drivers include DEM, slope and aspect, soil type, socio-economic factors such as population, GDP, nighttime light data, distance to highway exits (location information obtained from Gaode Map API), distance to national roads, provincial roads, railways, and main urban roads. Climate factors include annual average temperature and annual average precipitation. Using ArcGIS Pro, all data were unified to the WGS 1984 coordinate system at a resolution of 30 m. The InVEST water yield module requires precipitation data, potential evapotranspiration data, and soil datasets.

Data resolution and sources are shown in Table 1. Parameters for carbon storage and habitat quality are mainly derived from literature and repeated experiments [24].

Table 1. Descriptions of the data used in this paper.

Category	Data	Spatial Resolution	Data Source
CLCD	CLCD in 2001, 2011 and 2021	30 m	https://doi.org/10.5281/znodo.5816591 (Accessed: 22 January 2024)
Environmental driver	DEM	250 m	Resources and Environment Data Center, Chinese Academy of Sciences https://www.resdc.cn/data.aspx?DATAID=123 (Accessed: 22 January 2024)
	Soil type	1 km	Resources and Environment Data Center, Chinese Academy of Sciences https://www.resdc.cn/data.aspx?DATAID=145 (Accessed: 24 January 2024)
Socioeconomic driver	GDP	1 km	Resources and Environment Data Center, Chinese Academy of Sciences https://www.resdc.cn/DOI/DOI.aspx?DOIID=33 (Accessed: 24 January 2024)
	Population	1 km	Resources and Environment Data Center, Chinese Academy of Sciences https://www.resdc.cn/DOI/DOI.aspx?DOIID=32 (Accessed: 24 January 2024)
	Nighttime lighting big data	500 m	https://dataverse.harvard.edu/dataset.xhtml?persistentId=doi:10.7910/DVN/YGIVCD (Accessed: 24 January 2024)
	Distance to highway entrance and exit	30 m	Gaode OPEN API https://lbs.amap.com/ (Accessed: 28 January 2024)
	Distance to National Highway Distance to Provincial Highway Distance to railway Distance to primary roads	30 m	OpenStreetMap https://download.geofabrik.de/ (Accessed: 24 January 2024)
Climate driver	Annual mean temperature Annual mean precipitation	30 s	WorldClim https://www.worldclim.org/data/worldclim21.html (Accessed: 24 January 2024)
Water production service data	China's 1 km resolution monthly precipitation dataset (1901–2022) China's 1 km Monthly Potential Evapotranspiration Dataset (1901–2022)	1 km	National Earth System Science Data Center https://www.geodata.cn/main/ (Accessed: 16 May 2024)
	Chinese Soil Dataset Based on World Soil Database (HWSD) (v1.1)	1 km	National Glacier Frozen Soil Desert Science Data Center http://www.ncdc.ac.cn/portal/metadata/a948627d-4b71-4f68-b1b6-fe02e302af09 (Accessed: 16 May 2024)

3. Methods

In this study, the PLUS model was used for dynamic simulation and land use prediction. The predicted results were then imported into the InVEST model to calculate carbon storage, habitat quality, and water yield services based on the corresponding data.

The process of the PLUS model is as follows: land use data from 2001 to 2011, along with driver factor data, were input into the PLUS model to obtain the growth probability of each land use type and the simulated land use data for 2021. The accuracy was assessed by comparing the model output with actual land use data. After this, the Markov chain was used to calculate the land use demands for various types of land under different scenarios for 2031. Finally, the growth probabilities of each land use type and the land use types for 2031 under each scenario were input into the PLUS model using the 2021 land use data to generate the land use maps for 2031 under the Business-as-Usual Scenario (BS), Cropland Protection Scenario (CP), and Ecological Protection Scenario (EP). The General research framework is shown in Figure 1.

3.1. Future Urban Expansion Simulation

In this study, we selected CLCD data from 2001 to 2011 for the LXUA and used the LEAS module in the PLUS model to overlay the two periods of land use data. By using LEAS, we can obtain the conversion rules for all land use types to describe the nature of land changes over the same time interval (10 years) [25]. LEAS employs the Random Forest Classification (RFC) algorithm to transform the extraction of conversion rules for each land use type into a binary classification problem, with its formula as follows:

$$P_{i,k}^{d}(x) = \frac{\sum_{n=1}^{M} I(h_n(x) = d)}{M} \quad (1)$$

where $P_{i,k}^{d}$ is the growth probability of land use type k at cell i, and d is a value of 0 or 1. x is a vector composed of multiple driving factors. $I(\cdot)$ is the indicator function of the decision tree ensemble. $h_n(x)$ is the predicted type of the n-th decision tree for vector x. M is the total number of decision trees.

The PLUS model includes a CA model, which is a scenario-driven land use simulation model. During the simulation process, land use demand impacts local land use competition. To simulate the evolution of multiple land use type patches, the CA model uses a multi-type random patch seed mechanism based on threshold decline. This mechanism generates change "seeds" on each land use type's growth probability surface $P_{i,k}^{d=1}$ according to the overall probability. When considering neighborhood effects, the Monte Carlo method is used, employing pseudo-random numbers to simulate uncertainty under real-world conditions [26]:

$$OP_{i,k}^{d=1,t} = \begin{cases} P_{i,k}^{d=1} \times (r \times \mu_k) \times D_k^t \text{ if } \Omega_{i,k}^t = 0 \; and \; r < P_{i,k}^{d=1} \\ P_{i,k}^{d=1} \times \Omega_{i,k}^t \times D_k^t M \; all \; others \end{cases} \quad (2)$$

where $OP_{i,k}^{d=1,t}$ is the operation probability of land use type k at cell i and time t; r is a random value ranging from 0 to 1; μ_k is the threshold for generating new land use patches of type k; D_k^t is the diffusion coefficient of land use type; and $P_{i,k}^{d=1}$ is the growth probability of land use type k at time t.

To simulate land use in the study area under different development scenarios for 2031, it is first necessary to predict the land use demand for 2031 for each scenario. This is achieved by adjusting the Markov chain transition probabilities from 2011 to 2021 in the PLUS model. The principle of the Markov chain is as follows:

$$P_{ij} = \begin{bmatrix} P_{11} & P_{12} & \cdots & P_{1n} \\ P_{21} & P_{22} & \cdots & P_{2n} \\ \vdots & \vdots & \ddots & \vdots \\ P_{n1} & P_{n2} & \cdots & P_{nn} \end{bmatrix} and \sum_{j=1}^{n} P_{ij} = 1 (i, j = 1, 2, \cdots, n) \quad (3)$$

$$S_{t+1} = P_{ij} \times S_t \quad (4)$$

where S_t and S_{t+1} represent the land use states at time t and $t+1$, respectively, P_{ij} is the transition probability matrix, and n is the number of land use types.

This study constructs three development scenarios for the LXUA, including the Business-as-Usual Scenario (BS), the Cropland Protection Scenario (CP), and the Ecological Protection Scenario (EP). In the PLUS model, future land use pattern changing under different scenarios are predicted by modifying relevant parameters such as land use demand. Different transition probability matrices are set according to the land expansion, ecological restoration, and cropland preservation policies and planning intentions for the LXUA, as specified in actual planning documents and expert opinions. These documents include the "Lanzhou-Xining Urban Agglomeration Development Plan", "14th Five-Year Implementation Plan for Lanzhou-Xining Urban Agglomeration Development", " Qinghai Provincial Territorial Spatial Plan (2021–2035)", "Lanzhou City Territorial Spatial Master Plan (2020–2035)", "Xining City 14th Five-Year Plan for National Economic and Social Development and Long-term Goals for 2035", and "Lanzhou City 14th Five-Year Plan for National Economic and Social Development and Long-term Goals for 2035".

BS Scenario: Maintains the construction land expansion rate at the rapid urbanization level from 2011 to 2021, predicting using the actual land transfer probabilities obtained from the 2011 to 2021 land use analysis for the LXUA.

CP Scenario: The two modes of farmland protection in China are the first focusing on protecting the quantity and maintaining a dynamic balance of the total amount of farmland, and the second emphasizing the quality of farmland in basic farmland zoning. The former proposes the "compensation system for occupying arable land" based on the revised law of the Land Management Bureau in 1998 [8]. This law requires a balance between occupying and reclaiming arable land, which largely intervenes in the selection and direction of land use for urban expansion and rural construction. Moreover, it adopts the strictest cropland preservation measures according to relevant documents on cropland preservation

principles. The transfer matrix mainly reflects the quantity principle, thus reducing the actual transfer probability of cropland by 50%, while other land uses remain unchanged.

EP Scenario: Integrates the current ecological restoration policies from relevant documents, considering the applicability of ecological restoration policies to cropland, i.e., cropland ecosystems. The actual land transfer probabilities are adjusted by increasing the transfer probabilities from construction land and grassland to forest land by 10% and 20%, respectively. The transfer probabilities from cropland, forest land, grassland, and water bodies to construction land are reduced by 30%, 50%, 20%, and 20%, respectively, and the transfer probability from forest land to grassland is reduced by 50%.

Based on these, the land use demands under the three different scenarios were calculated using the Markov chain, and the specific quantities are shown in Table 2.

Table 2. The number of demand pixels of each land use type under different scenarios in 2031 (units: pixel).

Scenarios	Cropland	Forest	Shrub	Grassland	Water	Ice/Snow	Barren	Impervious	Wetland
2031 BS	15,183,787	4,019,626	1,085,004	81,248,948	4,507,132	1161	4,407,226	371,732	3237
2031 CP	16,829,985	4,012,748	1,085,013	79,641,506	4,499,563	1126	4,396,469	358,339	3100
2031 EP	15,187,162	4,145,506	1,086,840	81,135,045	4,507,244	1125	4,406,223	355,447	3263

Multiple indicators were used to validate the accuracy of the model simulation, including the *Kappa* index, *Overall Accuracy (OA)*, and the *Figure of Merit (FoM)*. The Kappa index detects the consistency of classification results in remote sensing images and is used here to test the consistency between the simulation results and the actual situation [27]. The methods for calculating these metrics are as follows:

$$kappa = \frac{OA_O - OA_E}{(1 - OA_E)}, OA_O = \frac{(\sum_{k=1}^{n} OA_{kk})}{N} \quad (5)$$

where OA_O is the overall accuracy of the classification, representing the probability that the simulated result of each random sample is consistent with the land use data; OA_E represents the probability that the simulated result matches the current land use data by chance; N is the total number of land use types, and n is the total number of samples; and OA_{kk} is the number of correctly classified samples for the k-th land use type. The *Kappa* coefficient ranges from -1 to 1, with higher values reflecting more accurate models.

$$FoM = B/(A + B + C + D) \times 100\% \quad (6)$$

where A is the error due to observed developed and simulated as persistence, B is the agreement due to observed developed and simulated as developed, C is the error due to observed developed and simulated as incorrect gaining category, and D is the error due to observed persistence and simulated as developed [28].

The LEAS module was used to obtain the development probabilities for each region in 2011 and 2021, and the CARS module was used to generate the simulated 2021 CLCD results for the LXUA. The simulated results were compared with the actual 2021 CLCD results, as shown in Figure 2. The comparison validated the accuracy of the PLUS model, yielding a *Kappa* coefficient of 0.82 and an Overall Accuracy of 0.90, both within the high-accuracy range [29]. The *FoM* value is approximately 0.72, indicating that the simulation achieved good cell-level agreement in this study [30]. Therefore, this model can be used to simulate the land use types of the LXUA for 2030.

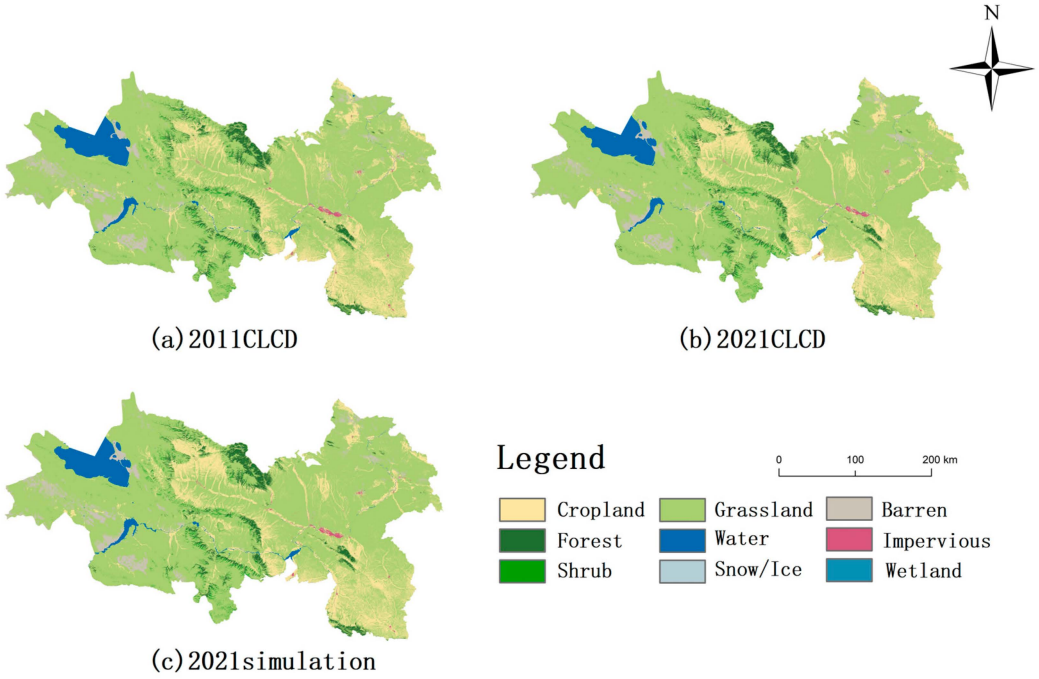

Figure 2. 2011, 2021 real CLCD, and 2021 simulated CLCD of the LXUA.

3.2. Carbon Storage

The carbon storage module in the InVEST model calculates carbon storage based on four fundamental carbon pools: aboveground biomass carbon (carbon contained in all living plants above the soil interface), belowground biomass carbon (carbon contained in living plant root systems below the soil interface), soil carbon (organic and mineral soil carbon within the soil itself), and dead organic matter carbon (carbon in plant litter and dead plants). According to the land use classification, the average carbon density of the aboveground carbon pool (C_{above}), belowground carbon pool (C_{below}), soil carbon pool (C_{soil}), and dead organic matter carbon pool (C_{dead}) for different land types is calculated. The total carbon storage (C_{total}) in the study area is then obtained by multiplying the area of each land type by its carbon density and summing the results [31]. The calculation formula is:

$$C_{total} = C_{above} + C_{below} + C_{soil} + C_{dead} \quad (7)$$

Based on the carbon density of each land type and land use data, the carbon storage of each land use type within the watershed is calculated as follows:

$$C_{totali} = (C_{above\ i} + C_{below\ i} + C_{soili\ i} + C_{dead\ i}) \times A_i \quad (8)$$

where i represents the average carbon density of each land use type, and A_i is the area of that land use type. The total carbon storage within the watershed is the sum of the carbon storage of all land types.

The carbon density data for different land use types were primarily obtained by referencing a large body of previous research [31–42]. The principle for selecting carbon density values prioritized using sampling point data from within the LXUA study area, followed by data from Qinghai and Gansu provinces. The carbon density table and literature sources are shown in Table 3.

Table 3. Carbon density and sources of different carbon storage.

Code	CLCD	Above	Below	Soil	Dead	Reference
1	Cropland	6.19	1.11	47.81	0	[31]
2	Forest	22.6	20.49	116.73	0	[32]
3	Shrub	1.9	6.2	94.6	0	[33,34]
4	Grassland	1	8.5	85.6	0	[35–39]
5	Water	0	0	39.8	0	[40]
6	Ice/Snow	0	0	0	0	[40]
7	Barren	0	2.1	13.44	0	[40]
8	Impervious	0	0	24.15	0	[40]
9	Wetland	1.5	15	44	0	[41,42]

3.3. Habitat Quality

Habitat quality refers to the capacity of a specific ecosystem to provide living and development conditions for organisms at a given time and place, making it an important indicator of the ecological environment in a region [43]. Different land use types provide different habitats for various species, and it is crucial to consider the impact of different threat sources on habitat quality. Before applying the InVEST model to calculate habitat quality in the LXUA, two factors must be considered.

Firstly, the distance between habitat grids and threat sources determines the attenuation of threat impacts. According to the InVEST model manual, spatially, this can be expressed using either a linear or exponential function [44]. The relationship between the threat impact and its distance from the habitat is as follows:

$$i_{rxy} = 1 - \left(\frac{d_{xy}}{d_{rmax}}\right) \; if \; linear \tag{9}$$

$$i_{rxy} = \exp\left(-\left(\frac{2.99}{d_{r\,\max}}\right) d_{xy}\right) if \; exponential \tag{10}$$

where d_{xy} is the linear distance between grids x and y, and d_{rmax} is the maximum effective distance of threat r.

Secondly, the relative sensitivity of different habitat types to threat sources must be considered. A habitat type that is more sensitive to a threat source is more likely to degrade under the influence of that threat [45]. The degree of habitat degradation is calculated as follows:

$$D_{xj} = \sum_{r=1}^{R} \sum_{y=1}^{Y_r} \left(\frac{w_r}{\sum_{r=1}^{R} w_r}\right) r_y i_{rxy} \beta_x S_{jr} \tag{11}$$

where D_{xj} is habitat degradation; R is the number of threat factors; Y_r is the number of grids corresponding to threat factor r; w_r and r_y are the weights and magnitude of the impact of threat r on the habitat; and β_x and S_{jr} represent the resilience and sensitivity of the habitat to the disturbance.

Based on the above, the habitat quality of the grid data can be calculated using the following formula:

$$Q_{xj} = H_j\left(1 - \left(\frac{D_{xj}^z}{D_{xj}^z + k^z}\right)\right) \tag{12}$$

where r is the grid, j is the habitat type, and Q is the habitat quality, ranging from 0 to 1; H_j is the habitat suitability; Z is a normalization constant; and k is the half-saturation parameter, set to the default value of 0.5 in this study.

In this study, based on existing research [43,46] and the classification of CLCD data selected in this paper, the threat factors, weights, and decay functions are shown in Table 4, while the habitat suitability and sensitivity to threat factors for different land uses are shown in Table 5.

Table 4. Threat factors and weights.

Threat	Max Distance/m	Weight	Decay
Cropland	4	0.6	Linear
Impervious	8	0.8	Exponential
Barren	6	0.5	Linear

Table 5. Habitat suitability and sensitivity to threat factors for each land class.

CLCD	Habitat Suitability	Cropland	Impervious	Barren
Cropland	0.5	0.0	0.6	0.4
Forest	0.9	0.6	0.8	0.2
Shrub	0.9	0.7	0.9	0.2
Grassland	0.75	0.7	0.7	0.7
Water	1.0	0.7	0.85	0.3
Ice/Snow	0.3	0.0	0.0	0.2
Barren	0.3	0.5	0.5	0.0
Impervious	0.1	0.1	0.0	0.1
Wetland	0.8	0.7	0.8	0.0

3.4. Water Yield

The water yield module is based on the Budyko water-energy coupling balance hypothesis formula and uses the annual average precipitation data for each unit grid to calculate the annual average water yield for each unit grid. This is done by taking the difference between the annual average precipitation and the annual actual evapotranspiration for each unit grid [47]. The formula is as follows:

$$Y_{xj} = \left(1 - \frac{AET_{xj}}{P_x}\right) \times P_x \tag{13}$$

where Y_{xj} and AET_{xj} represent the annual average water yield and the annual actual evapotranspiration for land use type j on grid cell x, respectively; P_x is the annual precipitation on grid cell x.

$$\frac{AET_x}{P_x} = \frac{1 + \omega_x + R_{xj}}{1 + \omega_x R_{xj} + \left(\frac{1}{R_{xj}}\right)} \tag{14}$$

$$\omega_x = Z \times \frac{AWC_x}{P_x} \tag{15}$$

$$R_{xj} = \frac{k_{ij} \times ET_0}{P_x} \tag{16}$$

where R_{xj} is the Budyko dryness index for land cover type j on grid cell x, ω_x is the ratio of the annual available water capacity to the expected precipitation, adjusted for vegetation; Z is the Zhang coefficient; AWC_x represents the soil available water content (mm), which determines the total amount of water stored and supplied by the soil for plant growth; and k_{ij} is the plant evapotranspiration coefficient [48].

$$AWC_x = \text{Min}(MSD_x, RD_x) \times PAWC_x \tag{17}$$

$$\begin{aligned} PAWC = {} & 54.509 - 0.132sand - 0.003\ sand^{\,2} - \\ & 0.055silt - 0.006\ silt^{\,2} - 0.738clay + 0.007\ clay^{\,2} - \\ & 2.688c + 0.501c^2 \end{aligned} \tag{18}$$

where MSD_x is the maximum soil depth; RD_x is the root depth; $PAWC$ is the plant available water content; sand, silt, and clay represent the content of sand, silt, and clay in the soil, respectively; and c is the soil organic carbon content.

In this study, the evaporation coefficients (Kc) and the maximum root depths for each land use type were determined according to the InVEST manual and reference values from the Food and Agriculture Organization (FAO), as shown in Table 6.

Table 6. Biophysical parameters of plants.

Land Use Code	Land Use Type	Maximum Root Depth (mm)	Kc
1	Cropland	2000	0.7
2	Forest	5200	1.0
3	Shrub	5200	0.95
4	Grassland	2600	0.85
5	Water	100	1.0
6	Ice/Snow	100	0.5
7	Barren	300	0.2
8	Impervious	100	0.3
9	Wetland	300	1.0

The Zhang coefficient is a crucial parameter in the water yield module, defining the fluctuation value of seasonal precipitation distribution and needs to be manually determined based on the characteristics of the study area. According to the "2022 Gansu Province Water Resources Bulletin" published by the government, the total water resources in the inland river basin are 5.013 billion cubic meters, with surface water resources amounting to 4.514 billion cubic meters and groundwater resources amounting to 3.978 billion cubic meters. The basin's water yield coefficient is 0.19. After running the model 30 times, it was found that when the Zhang coefficient is set to 1, the calculated water yield coefficient for 2021 is 0.195, which is closest to the actual water yield coefficient. Therefore, the Zhang coefficient is determined to be 1.

4. Results

4.1. Land Use Change in the LXUA from 2001 to 2021: Conflicts and Compromises Between Industrial Development, Ecological Protection, and Cropland Preservation

The LXUA experienced significant changes in land use from 2001 to 2021. As shown in Table 7, the land use in the LXUA in 2001, 2011, and 2021 was mainly concentrated in Grassland and Cropland. In 2001, Grassland accounted for 74.17% of the total land use area, and Cropland accounted for 14.75%. Forest, Shrub, Water, Barren, and Impervious land accounted for 2.97%, 1.1%, 3.46%, 3.35%, and 0.18%, respectively. Wetlands and Ice/Snow had smaller areas, both less than 0.01%. Over the next 20 years, significant changes occurred in various land use types.

Table 7. Land area and rate of change for different land types in the LXUA from 2001 to 2021.

Land Type	Area (km^2)			Change Rate		
	2001	2011	2021	2001–2011	2011–2021	2001–2021
Cropland	14,707.74	12,825.86	13,331.92	−12.8%	3.95%	−9.37%
Forest	2965.48	3151.95	3397.99	6.29%	7.81%	14.57%
Shrub	1105.56	1040.47	998.92	−5.89%	−4.06%	−9.63%
Grassland	73,985.41	75,754.85	74,285.44	2.39%	−1.94%	0.41%
Water	3454.65	3634.35	3838.85	5.20%	5.63%	11.11%
Ice/Snow	1.93	13.46	1.24	598.61%	−90.80%	−35.74%
Barren	3340.31	3072.12	3590.21	−8.03%	16.85%	7.49%
Impervious	183.40	251.23	294.27	37.00%	17.14%	60.48%
Wetland	0.57	0.78	2.09	36.94%	167.29%	266.06%

Over the past 20 years, driven by the urban expansion demands stimulated by industrial development, the protection of forest land under ecological protection policies and the quantitative requirements for cropland preservation, the land use changes in the LXUA

have demonstrated significant characteristics of policy intervention. Based on the changes in various typical land uses mentioned above, the objective changes in these typical land uses can be summarized with their policy causes, as shown in the following Table 8.

Table 8. Analysis of policy reasons for typical land cover changes in LXUA from 2001 to 2021.

Land Type	Trend	Policy Causes
Cropland	Cropland area significantly decreased from 14,707.74 km^2 in 2001 to 12,825.85 km^2 in 2011, then increased to 13,319.24 km^2 in 2021	Early urban expansion led to a large amount of rural land being converted to urban construction land. Later, the implementation of government cropland preservation policies and cropland reclamation projects led to an increase in cropland.
Forest	Forest area continuously increased over 20 years, from 2965.48 km^2 in 2001 to 3397.99 km^2 in 2021	Large-scale afforestation and ecological restoration projects implemented by the Chinese government, with forests given absolute priority in such projects.
Grassland	Grassland area first increased and then decreased, from 73,985.41 km^2 in 2001 to 75,754.85 km^2 in 2011, and then decreased to 74,285.44 km^2 in 2021	Early ecological protection projects like returning cropland to grassland increased grassland area, while later strict cropland protection policies led to grassland becoming a primary source for urban and rural construction land, causing a gradual decrease in area.
Impervious Land	Mainly urban construction land, its area continuously increased from 183.40 km^2 in 2001 to 294.27 km^2 in 2021	Direct reflection of urbanization. Support policies under the Western Development Strategy promoted urban construction and industrialization, leading to rapid urban expansion.

4.2. Analysis of 2031 Land Use Simulation Results

In the PLUS model, by adjusting the transition matrices and the neighborhood factor weight parameters for different scenarios, the 2021 CLCD data were used to predict land use for 2031. This resulted in the CLCD maps for different scenarios in 2031 (Figure 3), and the analysis of land use changes in the LXUA from 2001 to 2031 under different scenarios (Figure 4) along with the quantity table (Table 9). There are significant differences in the demand and distribution of land use types under different scenarios.

BS Scenario: This scenario simulates the natural evolution of land use in the LXUA based on the actual original transition probabilities. Under the BS scenario, Impervious land increases significantly by 13.96%, while Wetlands, Barren land, Forest, and Cropland increase by 39.71%, 10.48%, 6.46%, and 2.5%, respectively. In contrast, Ice/Snow, Grassland, and Shrub decrease by 15.56%, 1.56%, and 2.24%, respectively. The BS scenario effectively simulates the natural expansion trend of the urban agglomeration. Spatially, as shown in Figure 4, Impervious land improves the density within their original area while primarily expanding northward in Lanzhou City. The source of land for this expansion is mainly Grassland, supplemented by Cropland. In actual construction, the northward expansion trend of Lanzhou City corroborates this prediction, with new urban development areas such as Gaolan Ecological Restoration Demonstration Zone, Fuyuan New City, Qingbaishi Area, and Jiuzhou Area leading the development of Lanzhou's urban core. Ecologically, the changes in ecological land under the BS scenario have continued the trends observed in the past. Besides the growth in Forest and Barren land, Shrub and Grassland continue to decline, reflecting the natural recovery of forest and overused lands. Cropland shows a slight increase, continuing the trend of recovery and growth observed over the past decade.

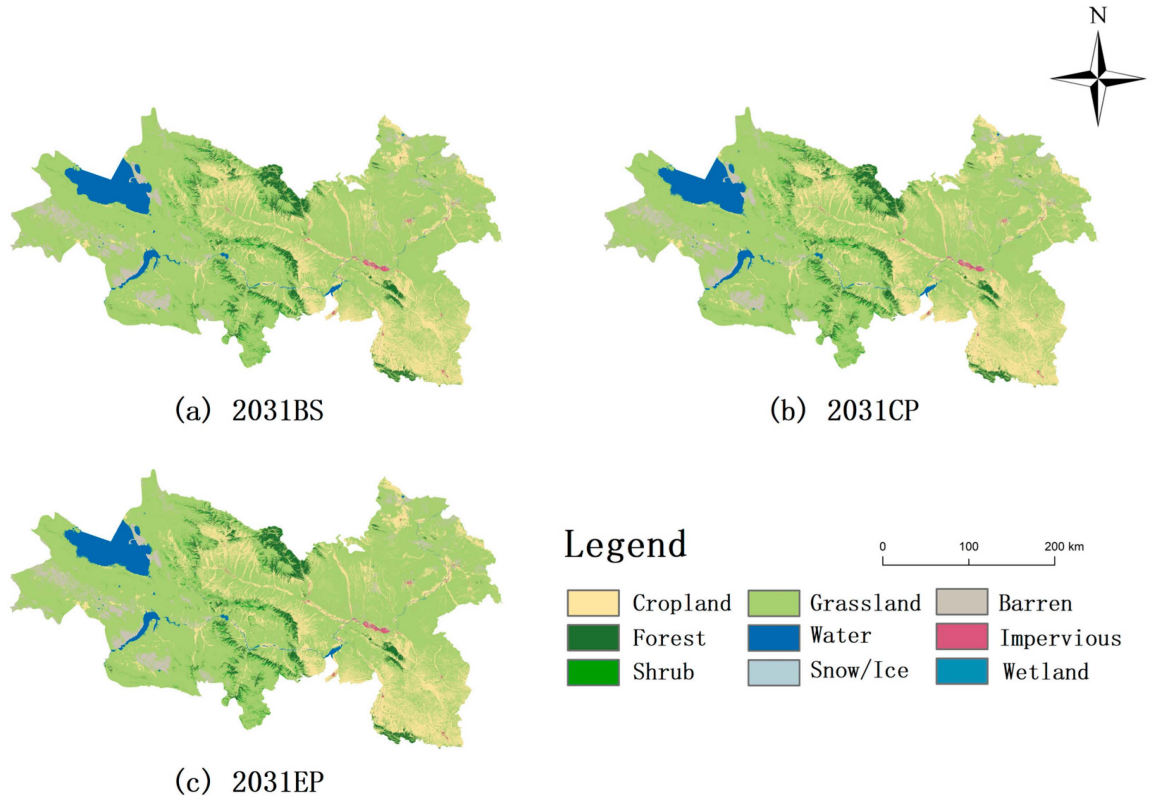

Figure 3. Land use simulation for different scenarios of the LXUA in 2031.

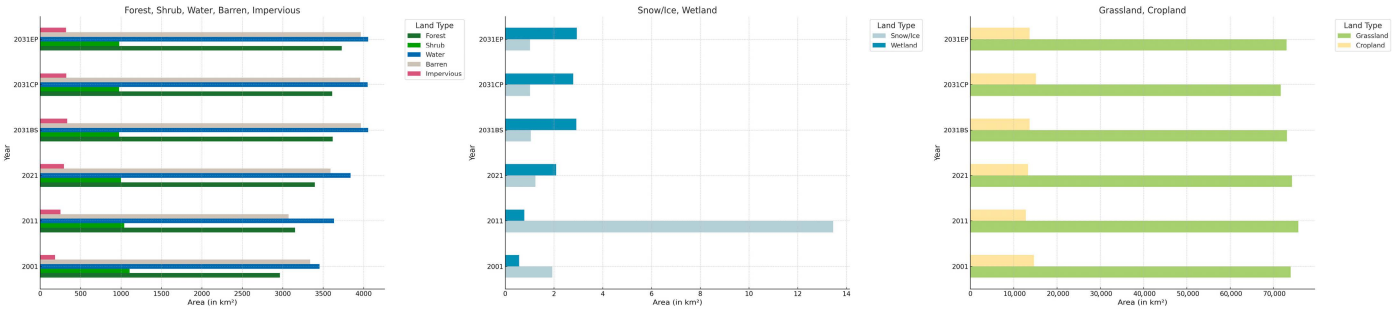

Figure 4. Land use change in the LXUA from 2001 to 2031.

CP Scenario: The Cropland Preservation Scenario strictly limits the conversion of cropland to other land types, reflecting the Chinese government's recent strict policies on cropland protection and food security. Under this scenario, cropland area increases by 1.81 km^2, a growth of 13.61% in quantity. Due to mandatory intervention policies, the amount of cropland in the LXUA has significantly increased in a short period. Nationally, while the eastern and southern regions lose large amounts of cropland due to economic development, the western regions, with abundant cropland resources, are increasingly important for national food security. The development of the LXUA under the CP scenario can undoubtedly lead to an increase in grain production in the West. However, this increase in cropland is spatially manifested as a delay in urban construction and more aggressive encroachment on grassland. The area of Impervious land under the CP scenario grows by 9.59%, which is equivalent to 70% of the Impervious land area growth under the BS scenario. Shrub and Grassland decrease by 2.24% and 3.5%, respectively. For Grassland, the area decrease under the CP scenario is 225% of that under the BS scenario, amounting to 2608.08 km^2. This will inevitably affect the local ecosystem services to some extent.

EP Scenario: Based on the existing policies of strict protection and management of forestry by the local government, the EP Scenario focuses on the protection of forest land. Under the EP Scenario, the growth areas of Forest and Wetlands are the highest among the three scenarios, with increases of 9.8% and 40.8%, respectively. The reduction in Shrub is the smallest among the three scenarios, at 2.07%. The growth area of Impervious land is also the lowest among the three scenarios, at 8.71%. Grassland decreases by 1.70%, and Cropland increases by 2.52%. The simulation of the EP Scenario achieves good results by sacrificing the urban construction land expansion rate while achieving significant growth in various ecological land types, reflecting a strong emphasis on the protection of different ecosystems.

Table 9. Land cover changes of LXUA under various scenarios from 2001 to 2031.

Year	Cropland	Forest	Shrub	Grassland	Water	Ice/Snow	Barren	Impervious	Wetland
2001	14.707.7442	2965.484	1105.5636	73.985.41	3454.655	1.926	3340.311	183.402	0.5697
2011	12.825.8568	3151.95	1040.4738	75.754.85	3634.348	13.4559	3072.125	251.2251	0.7803
2021	13.331.9241	3397.995	998.9217	74.285.44	3838.848	1.2375	3590.213	294.2739	2.0853
2031BS	13.665.4083	3617.663	976.5036	73.124.05	4056.419	1.0449	3966.503	334.5588	2.9133
2031CP	15.146.91301	3611.473	976.512145	71.677.36	4049.607	1.013446	3956.822	322.5058	2.790625
2031EP	13.668.44579	3730.955	978.155666	73.021.54	4056.519	1.013327	3965.6	319.9021	2.936272

4.3. Carbon Storage Analysis

From a temporal perspective, as shown in Figure 5a, the carbon storage in the LXUA was 8.6271×10^8, 8.7194×10^8, and 8.6599×10^8 t in 2001, 2011, and 2021, respectively, with average carbon densities of 86.4910 t/ha, 87.4166 t/ha, and 86.8241 t/ha. The carbon storage in 2031 under the BS, CP, and EP scenarios was 8.6126×10^8 t, 8.5585×10^8 t, and 8.6245×10^8 t, with average carbon densities of 86.3821 t/ha, 85.8039 t/ha, and 86.4656 t/ha, respectively. Compared to 2021, the carbon storage in 2031 showed a declining trend under the BS, CP, and EP scenarios, with decreases of 0.5%, 1.17%, and 0.41%, respectively. The significant increase in Cropland is the main reason for the fastest decline in carbon storage under the CP scenario, while the increase in Forest area is the reason for the smallest loss in carbon storage under the EP scenario. From the perspective of different land use types, as shown in Figure 5b, Grassland and Cropland account for the largest share of carbon storage, comprising over 85% of the total carbon storage, and the overall trend of carbon storage changes aligns with the changes in Grassland area. Among the various years, the carbon storage of Cropland under the CP scenario in 2031 is the highest, accounting for 15.18% of the total carbon storage for that period.

There is also significant spatial heterogeneity in ecosystem carbon storage. As shown in Figure 6, the area with low carbon storage is mainly located in the Gonghe Basin to the southwest of the boundary marked by Qinghai Nanshan, Laji Mountain, and Jishi Mountain. This region has high altitudes and low temperatures, and is dry due to air currents being blocked by the surrounding uplifts, making it unsuitable for vegetation growth. The area east of the boundary has higher carbon storage. The differences in carbon storage are mainly due to differences in land use types, with the lowest areas dominated by Barren and Impervious land, and the lower areas mainly consisting of Cropland. Additionally, some areas east of Qinghai Lake have lower carbon storage due to the blockage by Riyue Mountain on the east side, causing wind-borne sand to settle and accumulate, leading to desertification and reduced vegetation growth, thereby reducing carbon sequestration. The same principle applies to small areas with lower carbon storage in the northeast uplifted terrain. Overall, the distribution of carbon storage is greatly influenced by topography and land use types.

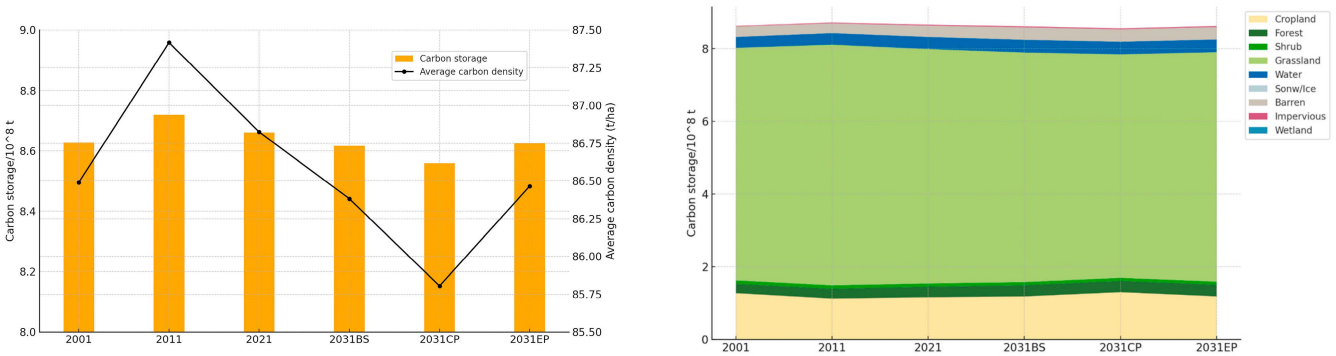

(**a**) (**b**)

Figure 5. (**a**): Carbon storage and average carbon density changes in the LXUA from 2001 to 2031; (**b**): Changes in carbon storage of different land use types in the LXUA from 2001 to 2031.

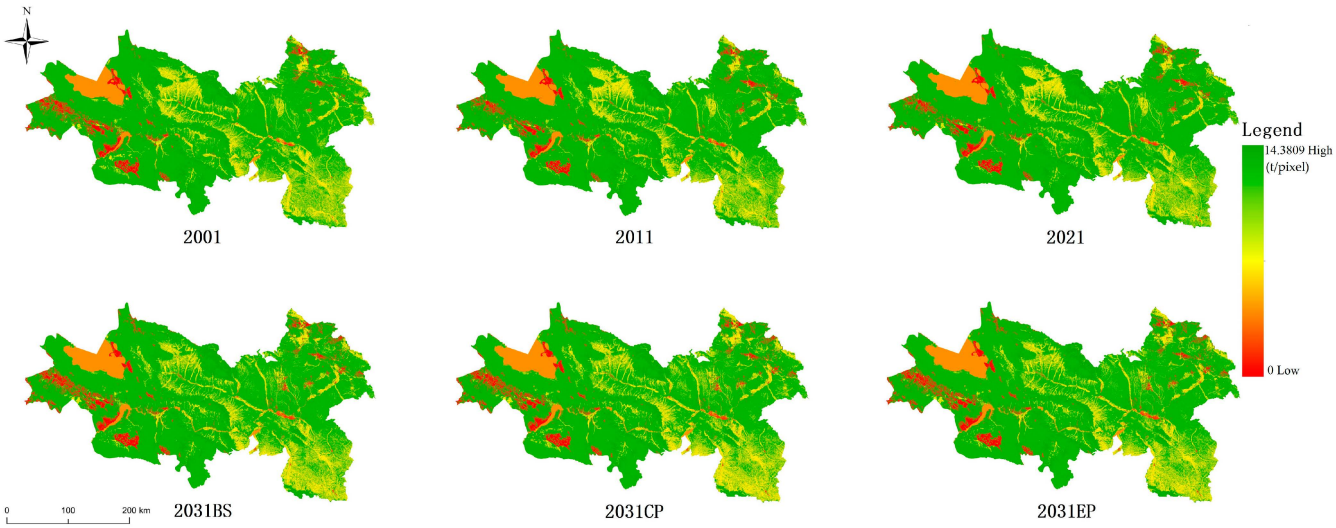

Figure 6. Changes in carbon storage of different land use types in the LXUA from 2001 to 2031.

4.4. Habitat Quality Analysis

The average habitat quality in 2001, 2011, and 2021 was 0.7130, while the simulated average habitat quality in 2031 for the three scenarios was 0.7098, indicating a decline (Table 10). Spatially, habitat quality was divided into five levels: low (0–0.2), relatively low (0.2–0.4), medium (0.4–0.6), relatively high (0.6–0.8), and high (0.8–1), as shown in Figure 7. The spatial distribution of habitat quality is closely related to land use, with high-quality areas concentrated in Forest and Water, relatively high-quality areas in Grassland, medium-quality areas in Cropland, relatively low-quality areas in Barren, and low-quality areas in Impervious land.

As shown in Figure 7, the spatial expansion of Cropland and Impervious land has resulted in the fragmentation and isolation of relatively high-quality Grassland, forming dense patches in the southeast and central parts of the study area. Some of these patches are connected to other Grasslands, while others are completely isolated, surrounded by medium-quality Cropland and low-quality Impervious land, forming numerous patches or biological islands of varying sizes. According to island biogeography and related theories, more isolated patches have lower species migration rates, and smaller patches have higher extinction rates compared to larger patches [49]. In the LXUA, these biological islands are primarily due to the intersection and fragmentation caused by expanding Cropland and encroaching Grassland. Among the various future scenarios, the 2031 CP scenario, with the

highest proportion of Cropland, has the most isolated islands. This situation may accelerate species extinction within the islands, thereby affecting the overall habitat quality.

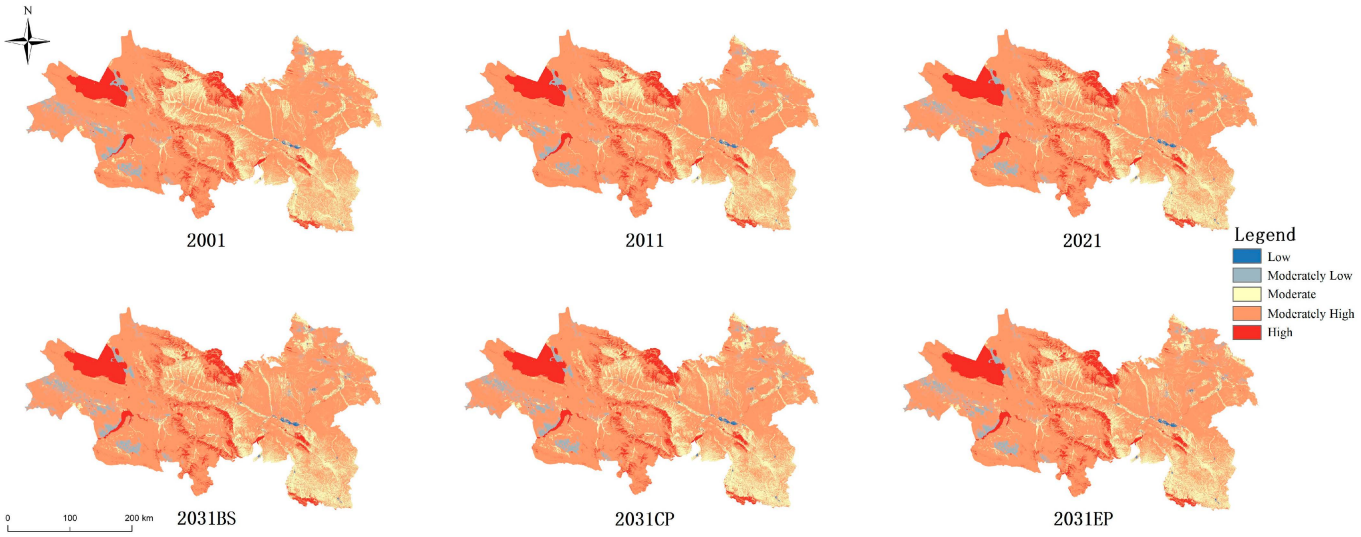

Figure 7. Spatial distribution of habitat quality in the LXUA from 2001 to 2031.

Temporally, from 2001 to 2021, the average habitat quality initially increased by 0.0063 and then decreased by 0.0031. Analyzing the land use changes, this fluctuation is attributed to the initial increase and subsequent decrease in cropland driven by policy interventions. Overall, the average habitat quality in 2021 increased by 0.0032 compared to 2001, reflecting the positive impact of ongoing ecological restoration policies by local governments.

Under the simulated scenarios, the average habitat quality in 2031 under the CP scenario is the lowest, falling below the 2001 level. This decline is due to the disorderly expansion of Cropland, which undermined local habitats and negated 20 years of ecological restoration efforts. Among the three scenarios, the highest average habitat quality is under the 2031 EP scenario, with a value of 0.7712, still below the 2021 level. In 2031, the amount of Impervious land increases across all scenarios. Despite aggressive ecological protection policies resulting in the highest forest area in 30 years, the overall ecological quality still declines. This decline is likely due to the significant impact of Impervious land expansion on habitat quality, warranting further investigation into the specific extent of this impact.

Table 10. Average habitat quality from 2001 to 2031.

Year	Average Habitat Quality
2001	0.7098
2011	0.7161
2021	0.7130
2031BS	0.7110
2031CP	0.7072
2031EP	0.7112

4.5. Water Yield Analysis

Water yield values depend on local precipitation, actual evapotranspiration, and the balance between the two. As precipitation is an uncontrollable variable, this study uses 2021 precipitation data, focusing on the spatial distribution of water yield and evapotranspiration to uncover their spatial characteristics. For the western regions with low precipitation, snowmelt becomes the main source of water yield in the LXUA.

From the spatiotemporal distribution, as shown in Figure 8a, areas with relatively high water yield are mainly concentrated in the high mountain snowline areas in the northwest

of the study area. These regions, relying on snowmelt, have sufficient water replenishment, greatly exceeding evapotranspiration, resulting in high water yield. Apart from these areas, the rest of the region has a balanced but low water yield.

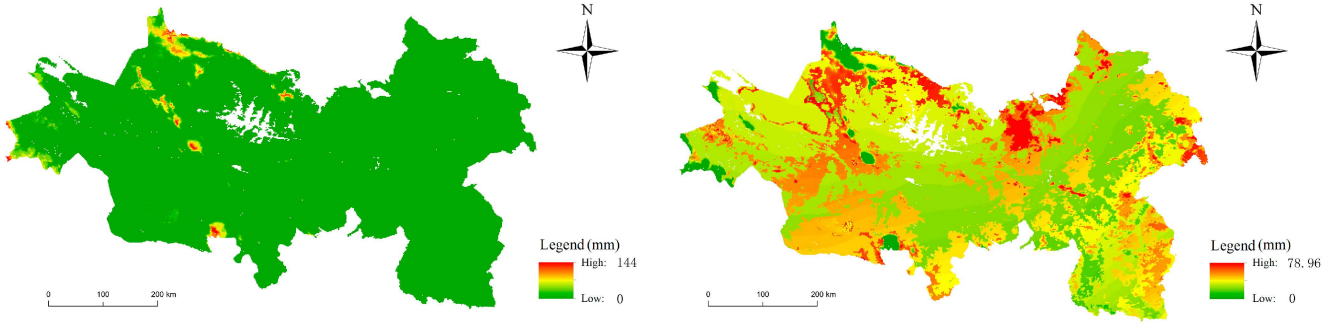

(**a**) (**b**)

Figure 8. (**a**) Spatial distribution of water yield. (**b**) Spatial distribution of evaporation.

Regarding evapotranspiration, as shown in Figure 8b, areas with lower evapotranspiration are mainly concentrated on the southern side of Laji Mountain, the two sides of the mountains southeast of Qinghai Lake and the northeastern part of the LXUA along the Yellow River, which are currently dominated by Cropland and Grassland. The region with the lowest evapotranspiration is the high water yield snowline area, currently dominated by Barren and Grassland. High evapotranspiration areas highly overlap with the spatial distribution of Impervious land. Additionally, the northern part of the LXUA is a dense high evapotranspiration area. Overall, evapotranspiration in the urban agglomeration is characterized by high values in the north and south and low values in the center.

5. Discussion and Conclusions

5.1. Discussion

5.1.1. How Will the LXUA Expand by 2031?

Under the current background of various Chinese policies such as cropland balance, total forest area balance, and rural revitalization, the expansion of Impervious land in the LXUA is the driving force behind the adjustment of the entire urban agglomeration's land use structure. The expansion of Impervious land in the LXUA is the result of the complex effects of the Western Development Strategy and various policies. The direction of this expansion implies the future spatial trends and patterns of the urban agglomeration.

Using the PLUS model, this study simulates the land use in the LXUA under three scenarios in 2031 and attempts to explore the patterns of Impervious land and various land use changes. The amount of Impervious land in three scenarios in 2031 continues to increase, indicating that the demand for urban development and expansion persists. From the spatial distribution perspective, combining the expansion patterns of the past 20 years, the expansion of patches under all three scenarios mainly involves increasing the density of existing Impervious land patches in Lanzhou City and Xining City, while the Impervious land patches led by Lanzhou City expand northward. The main sources of this land are Grassland, followed by Cropland. The expansion of Impervious land patches is most pronounced under the BS scenario and least pronounced under the EP scenario. The simulated expansion patterns of Impervious land align with the current actual "northward expansion" planning scheme of Lanzhou City.

5.1.2. How Will Multiple Scenarios Affect Ecosystem Services in the LXUA?

Based on the analysis and simulation of land use and Impervious land expansion in the LXUA, different expansion scenarios and varying degrees of policy intervention influence the urban agglomeration's ecosystem services. Unlike traditional single land

use raster data analysis methods, this study uses the InVEST model and multi-source data to measure the quantitative values and spatial distribution of three important ecosystem services in the LXUA. The study results indicate a close relationship between land use and ecosystem services in the LXUA. The impacts on the three types of ecosystem services are summarized as follows:

Carbon Storage: Land use affects carbon density changes, thereby impacting overall carbon storage. All three future scenarios show a loss in carbon storage compared to 2021. Among them, the EP scenario has the highest carbon storage, while the CP scenario has the lowest. This reflects the loss in carbon storage due to the increase in Cropland and the importance of increasing Forest and Grassland areas for carbon storage.

Habitat Quality: The spatial distribution of habitat quality is closely related to land use. Impervious land, as the sole source of low habitat quality, significantly affects the overall habitat quality of the urban agglomeration. Additionally, as the two largest land types in the LXUA, Grassland has higher habitat quality than Cropland. Therefore, the balance between these two areas also affects the overall habitat quality. In the zones where Grassland and Cropland intermingle, biological islands are prone to form. In all three future scenarios, the average habitat quality declines, with the EP scenario having the highest average habitat quality at 0.7112, and the BS scenario having the lowest at 0.7072. This underscores the detrimental impact of disordered Cropland expansion on existing habitats.

Water Yield: Due to the geographical location of the LXUA, which has low precipitation, the high water yield is concentrated in the high mountain snow areas within the LXUA. The spatial distribution of Impervious land overlaps with high evapotranspiration areas. The increase in Impervious land directly affects the evapotranspiration in the LXUA. Additionally, the uneven spatial distribution of water yield presents limitations for the urban agglomeration's development.

5.1.3. Policy Implications

(1) Allowing "Breathing" Space for Land Expansion in the LXUA

Based on the previous calculations of carbon storage and habitat quality, the average carbon storage and habitat quality of Grassland in the LXUA are higher than those of Cropland. From the past land use changes in the LXUA, we observe close land use conversions between Grassland and Cropland, with the growth of Impervious land mainly sourced from Grassland and Cropland. In all three future scenarios, whether emphasizing the increase in Cropland in the CP scenario, the increase in Forest in the EP scenario, or the fastest growth of Impervious land in the BS scenario, the growth sources will predominantly occupy large areas of Grassland. Even though this trend and the amount of occupation are unavoidable, we can still mitigate the impact on habitat quality and carbon storage through the following spatial expansion measures:

Firstly, Cropland protection should leave ecological corridors to prevent habitat fragmentation and improve carbon sequestration. According to the theory of ecological corridors, these are channels connecting separated habitat patches, allowing species to migrate and interact between different habitats. This helps maintain biodiversity and prevents the negative impacts of habitat fragmentation. During the inevitable process of increasing Cropland and encroaching on Grassland, it is crucial to prevent the formation of isolated habitat islands. Leaving corridors to connect the surrounding Grassland with external ecological spaces can enhance the habitat quality of these Grasslands. Additionally, using the root systems of Grassland to increase the organic carbon content of the land can promote the increase and stability of carbon storage.

Secondly, Impervious land expansion should focus on integrating boundaries with natural spaces. In the process of urban agglomeration expansion, it is important to avoid cutting off ecological corridors entirely. On a large spatial scale, the role of corridors within the land use should be emphasized. Wherever possible, existing urban agglomerations should circumvent or avoid corridors. Moreover, within the existing urban land, efforts should be made to connect internal Grassland or Forest areas with external eco-

logical networks, transforming these Grasslands into extensions of the external ecological environment, thereby enhancing their resilience and habitat quality.

In a word, by leaving "breathing" spaces in both the growth of Cropland and the expansion of Impervious land, it is possible to improve ecological quality while stabilizing carbon storage, thus enhancing the ecosystem services of the LXUA.

(2) Creating a Cross-Provincial "Ecological Network" for Future Ecological Red Line Delineation in the LXUA

Currently, China implements a strict ecological red line system to guide the expansion of urban agglomerations. The ecological protection red line delineates spatial boundaries and management limits that require stringent protection in terms of natural ecological service functions, environmental quality safety, and natural resource utilization. This aims to maintain national and regional ecological security, ensure sustainable economic and social development, and protect public health [50]. The ecological red line significantly impacts the improvement and enhancement of ecosystem service functions.

Presently, the ecological protection red line is implemented on a provincial basis. In practice, isolated ecological red line areas are delineated based on regions with significant ecological functions and high sensitivity within different provinces. To enhance the overall ecosystem services of the LXUA, it is crucial to transcend the administrative boundaries of Qinghai Province and Gansu Province and coordinate the tasks of ecological protection and development of the urban agglomeration. Considering the regional ecological red line from a broader perspective becomes particularly important.

Cross-administrative ecological red line delineation should establish a large-scale ecological network. Based on the findings of this study, there is room for further improvement within the current patch-based system. From the spatial perspective of the urban agglomeration, the ecosystem services of smaller patches can significantly impact the entire urban area. For example, high water yield primarily comes from small snow-covered areas, and high habitat quality is influenced by relatively small forested areas. These scattered small patches bear substantial ecosystem service functions. In the patch-based system, planners often overlook the connections between patches. Although the short-term impacts of this oversight may not be noticeable, in the long-term urban expansion, these isolated small patches may fail to provide their original ecosystem services and functions, potentially causing irreversible damage to the overall ecosystem services of the urban agglomeration.

Therefore, in the future development of urban agglomerations, the delineation of ecological red lines should not only focus on protecting areas with strong ecological functions and high sensitivity but also on maintaining the corridors between these large patches and adjacent small patches. Even if these corridors themselves have low functionality, sensitivity, and small areas, they are essential for the smooth flow and exchange of various substances and energy between patches. This facilitates better performance of ecological services and functions by each patch. Establishing a giant ecological network across the LXUA spanning the two provinces is expected to generate better overall ecological effects and drive regional ecological environmental improvements.

(3) Reassessing the Timeline for Well-Facilitated Cropland Construction in the LXUA from an Ecosystem Services Perspective

Cropland preservation is the policy direction for the expansion of impervious land in the LXUA. The "Gansu Province Territorial Spatial Planning (2021–2035)" states that the province's cropland preservation should be no less than 5.13 million ha, with no less than 4.25 million ha of permanent basic cropland protection. Beyond emphasizing cropland quantity control, improving cropland quality is crucial, with well-facilitated cropland construction being the primary measure for enhancing cropland quality in China. According to the "General Rules for Well-Facilitated Cropland Construction" [51] (GB/T30600-2022) released by China, well-facilitated cropland refers to land that is flat, contiguous, well-equipped with facilities, and suitable for modern agricultural production and management methods. It is high-yield and stable, with good ecological conditions and strong disaster

resistance, and is designated as permanent basic cropland. Nationally, well-facilitated cropland increases per-mu grain production capacity by 10–20%, saves water and fertilizer, enhances disaster resilience, and is suitable for mechanized operations and large-scale management, promoting cost savings and income growth for farmers. However, the construction of well-facilitated cropland requires significant investment, directly affecting construction standards and quality. Currently, the average construction cost per mu in China is generally 3000 yuan, exceeding 5000 yuan in hilly areas, not including maintenance costs. In addition, the "National Well-Facilitated Cropland Construction Plan (2021–2030)" outlines regional construction priorities. For the northwest and Qinghai-Tibet regions, where the LXUA is located, the focus is on improving field irrigation and drainage facilities, promoting efficient water-saving irrigation methods such as drip, sprinkler, and micro-irrigation, and increasing water resource utilization efficiency. The irrigation guarantee rate of well-facilitated cropland should reach over 50%. In addition, specific requirements are set for per-mu yield, soil organic matter, soil pH, cultivation layer thickness, and road network density, with specific measures for land leveling, infrastructure, and ecological restoration [52].

How can the construction of well-facilitated cropland be promoted to enhance the overall cropland quality in the LXUA? The authors believe that approaching well-facilitated cropland construction from an ecosystem services perspective may yield unexpected benefits. Currently, areas with good natural conditions and high economic returns, particularly rural areas with large amounts of leased land, are prioritized for construction due to higher investment returns and strong self-financing capabilities among the local population and capital. However, poorer rural areas may struggle to afford the initial costs of well-facilitated cropland construction, and even if built, insufficient investment may lead to formalism, emphasizing land leveling with poor subsequent results and sustainability. For these areas, the government can take a more macro and long-term approach, prioritizing well-facilitated cropland construction in areas with low evapotranspiration, high habitat quality, and high carbon storage. This can maximize the benefits of limited financial expenditure by improving the construction sequence. Although these areas mainly consist of dry land with poor infrastructure and low-yield benefits before construction, they have great potential. Implementing water-saving irrigation and other well-facilitated cropland construction measures in these areas may be highly effective.

Given the geographic environment of the LXUA, enhancing cropland quality involves reducing future irrigation costs and increasing water conservation capacity due to low evapotranspiration. High habitat quality indicates stronger cropland ecosystem functions, greater resilience, and better suitability for crop growth with the same investment. High carbon storage implies higher soil organic matter content and greater soil fertility potential. From an ecological perspective, this dual benefit promotes cropland protection and ecological restoration, further improving cropland habitat quality and benefiting surrounding forests and water bodies. This approach fosters the development of surrounding environments, drives spontaneous ecological construction by farmers, and promotes a positive cycle for the regional ecosystem, enhancing ecosystem services while reducing ecological restoration costs. From a socio-economical perspective, well-facilitated cropland construction that prioritizes long-term gains and equitable distribution can enhance both cropland and ecological quality, allowing potential-rich cropland to thrive and benefiting more rural impoverished areas. This ensures that the policy investment does not exacerbate the Matthew effect.

5.2. Conclusions

Taking the LXUA as a study case, this paper follows the "history-present-future" logical framework. In addition, the PLUS model and InVEST model were used to construct three future scenarios for the modernization stage in 2031 dominated by different land use policies in this study. This provides an integrated assessment framework that comprehensively considers the impact of urban expansion, cropland preservation, and

ecological protection on ecosystem services, and proposes coordinated suggestions to promote regional sustainable development. The following conclusions are drawn: (1) The land use changes from 2001 to 2021 reflect the impacts and conflicts among the Western Development Strategy, ecological protection policies, and cropland preservation policies. (2) In 2031, construction land continues to increase under all three scenarios, expanding northwards around Lanzhou, consistent with the actual "northward expansion" trend of Lanzhou City. Changes in other land uses are in line with the directions guided by land use policy. (3) By 2031, carbon storage and habitat quality decline under all scenarios, with the highest values observed in the EP scenario, the lowest carbon storage in the BS scenario, and the lowest habitat quality in the CP scenario. Regarding water yield, the LXUA primarily relies on alpine snowmelt, with construction land overlapping high evapotranspiration areas. (4) Based on the assessment of ecosystem services, urban expansion, delineation of ecological red lines and improvement of cropland quality in the LXUA were proposed. These findings and recommendations can provide a scientific basis for policymakers and planning managers in future.

Author Contributions: Conceptualization, Z.G.; Methodology, Z.G. and W.L.; Resources, Z.G. and Y.S.; Data curation, Z.G. and Y.G.; Writing—original draft, Z.G. and J.R.; Writing—review and editing, J.R. and J.G.; Supervision, J.R. and W.B.; Project administration, J.R. and C.L. All authors have read and agreed to the published version of the manuscript.

Funding: This study was supported by the National Social Science Foundation Youth Project of China (21CGL040); the Qinghai Provincial Social Science Foundation Youth Project (23Q060); the Open Research Fund Program of Laboratory for Ecological Protection and High-quality Development of the Upstream of Yellow River (2024hhsy04).

Data Availability Statement: The data presented in this study are available from the corresponding author upon request.

Conflicts of Interest: The authors declare that they have no known competing interests.

References

1. Zhang, Z.X.; Li, Y.; Wang, X.G.; Zhu, L.; Li, H.Z.; Liu, Y.; Tang, N.B.; Xu, Y.; Hu, Q.Y. Investigating River Health and Potential Risks Using a Novel Hybrid Decision-Making Framework with Multi-Source Data Fusion in the Qinghai-Tibet Plateau. *Environ. Impact Assess. Rev.* **2022**, *96*, 106849. [CrossRef]
2. China Keywords. Available online: http://keywords.china.org.cn/m/2022-07/11/content_78317142.html (accessed on 30 June 2024). (In Chinese)
3. Kong, Y.; He, W.J.; Qin, Z.H.; Tan, J.T. Net Effect Evaluation on China's Western Development Policy. *Stat. Decis.* **2018**, *34*, 91–95. (In Chinese)
4. Lu, F.; Hu, H.F.; Sun, W.J.; Zhu, J.J.; Liu, G.B.; Zhou, W.M.; Zhang, Q.F.; Shi, P.L.; Liu, X.P.; Wu, X.; et al. Effects of National Ecological Restoration Projects on Carbon Sequestration in China from 2001 to 2010. *Proc. Natl. Acad. Sci. USA* **2018**, *115*, 4039–4044. [CrossRef]
5. Xiao, L.L.; Yang, X.H.; Cai, H.Y.; Zhang, D.X. Cultivated Land Changes and Agricultural Potential Productivity in Mainland China. *Sustainability* **2015**, *7*, 11893–11908. [CrossRef]
6. Bennett, M.T. China's Sloping Land Conversion Program: Institutional Innovation or Business as Usual? *Ecol. Econ.* **2008**, *65*, 699–711. [CrossRef]
7. Research Group of National Bureau of Statistics. The Impact of "cropland Re-turning into Forest" upon Grain Production, Supply and Demand in West China. *J. Manag. World* **2004**, *20*, 97–100+108. (In Chinese)
8. Wu, Y.Z.; Shan, L.P.; Guo, Z.; Peng, Y. Cultivated Land Protection Policies in China Facing 2030: Dynamic Balance System versus Basic cropland Zoning. *Habitat Int.* **2017**, *69*, 126–138. [CrossRef]
9. Reid, W.V.; Mooney, H.A.; Cropper, A.; Capistrano, D.; Carpenter, S.R.; Chopra, K.; Dasgupta, P.; Dietz, T.; Duraiappah, A.K.; Hassan, R.; et al. *Millennium Ecosystem Assessment: Ecosystems and Human Well-Being*; Island Press: Washington, DC, USA, 2005.
10. Qiu, H.H.; Hu, B.Q.; Zhang, Z. Study on Ecosystem Service Value of Guangxi in the Past 20 Years Based on Land Use Change. *J. Environ. Eng. Technol.* **2022**, *12*, 1455–1465. (In Chinese)
11. Fu, B.J.; Zhang, L.W. Land-use Change and Ecosystem Services: Concepts, Methods and Progress. *Prog. Geogr.* **2014**, *33*, 441–446. (In Chinese)
12. Maimaiti, B.; Chen, S.S.; Kasimu, A.; Mamat, A.; Aierken, N.; Chen, Q.L. Coupling and Coordination Relationships between Urban Expansion and Ecosystem Service Value in Kashgar City. *Remote Sens.* **2022**, *14*, 2557. [CrossRef]

13. Fu, B.J.; Wang, S.; Su, C.H.; Forsius, M. Linking Ecosystem Processes and Ecosystem Services. *Curr. Opin. Environ. Sustain.* **2013**, *5*, 4–10. [CrossRef]
14. Troy, A.; Wilson, M.A. Mapping Ecosystem Services: Practical Challenges and Opportunities in Linking GIS and Value Transfer. *Ecol. Econ.* **2006**, *60*, 435–449. [CrossRef]
15. Liang, X.; Guan, Q.F.; Clarke, K.C.; Liu, S.S.; Wang, B.Y.; Yao, Y. Understanding the Drivers of Sustainable Land Expansion Using a Patch-generating Land Use Simulation (PLUS) Model: A Case Study in Wuhan, China. *Comput. Environ. Urban Syst.* **2021**, *85*, 101569. [CrossRef]
16. Wang, Z.; Zeng, J.; Chen, W.X. Impact of Urban Expansion on Carbon Storage under Multi-Scenario Simulations in Wuhan, China. *Environ. Sci. Pollut. Res.* **2022**, *29*, 45507–45526.
17. Li, Y.H.; Yao, S.; Jiang, H.Z.; Wang, H.R.; Ran, Q.C.; Gao, X.Y.; Ding, X.Y.; Ge, D.D. Spatial- Temporal Evolution and Prediction of Carbon Storage: An Integrated Framework Based on the MOP–PLUS–InVEST Model and an Applied Case Study in Hangzhou, East China. *Land* **2022**, *11*, 2213. [CrossRef]
18. Anjinho, P.D.S.; Barbosa, M.A.G.A.; Mauad, F.F. Evaluation of InVEST's Water Ecosystem Service Models in a Brazilian Subtropical Basin. *Water* **2022**, *14*, 1559. [CrossRef]
19. Louis, V.; Page, S.E.; Tansey, K.J.; Jones, L.; Bika, K.; Balzter, H. Tiger Habitat Quality Modelling in Malaysia with Sentinel-2 and InVEST. *Remote Sens.* **2024**, *16*, 284. [CrossRef]
20. Arsanjani, J.J.; Helbich, M.; Kainz, W.; Boloorani, A.D. Integration of Logistic Regression, Markov Chain and Cellular Automata Models to Simulate Urban Expansion. *Int. J. Appl. Earth Observ. Geoinform.* **2013**, *21*, 265–275. [CrossRef]
21. Adnan, M.S.G.; Abdullah, A.Y.M.; Dewan, A.; Hall, J.W. The Effects of Changing Land Use and Flood Hazard on Poverty in Coastal Bangladesh. *Land Use Policy* **2020**, *99*, 104868.
22. Halmy, M.W.A.; Gessler, P.E.; Hicke, J.A.; Salem, B.B. Land Use/Land Cover Change Detection and Prediction in the North-Western Coastal Desert of Egypt Using Markov-CA. *Appl. Geogr.* **2015**, *63*, 101–112.
23. Yang, J.; Huang, X. The 30 m Annual Land Cover Dataset and Its Dynamics in China from 1990 to 2019. *Earth Syst. Sci. Data* **2021**, *13*, 3907–3925. [CrossRef]
24. Ren, J.; Ma, R.R.; Huang, Y.H.; Wang, Q.X.; Guo, J.; Li, C.Y.; Zhou, W. Identifying the Trade-Offs and Synergies of Land Use Functions and Their Influencing Factors of Lanzhou-Xining Urban Agglomeration in the Upper Reaches of Yellow River Basin, China. *Ecol. Indic.* **2024**, *158*, 111279.
25. Liang, X.; Liu, X.P.; Li, D.; Zhao, H.; Chen, G.Z. Urban Growth Simulation by Incorporating Planning Policies into a CA-Based Future Land-Use Simulation Model. *Int. J. Geogr. Inform. Sci.* **2018**, *32*, 2294–2316. [CrossRef]
26. Liu, X.P.; Liang, X.; Li, X.; Xu, X.C.; Ou, J.P.; Chen, Y.M.; Li, S.Y.; Wang, S.J.; Pei, F.S. A Future Land Use Simulation Model (FLUS) for Simulating Multiple Land Use Scenarios by Coupling Human and Natural Effects. *Landsc. Urban Plan.* **2017**, *168*, 94–116.
27. Shi, X.; Wu, L.; Zheng, Y.Q.; Zhang, X.; Wang, Y.J.; Chen, Q.; Sun, Z.Y.; Nie, T.Z. Dynamic Estimation of Mangrove Carbon Storage in Hainan Island Based on the InVEST-PLUS Model. *Forests* **2024**, *15*, 750.
28. Chen, Y.M.; Li, X.; Liu, X.P.; Ai, B. Modeling Urban Land-Use Dynamics in a Fast Developing City Using the Modified Logistic Cellular Automaton with a Patch-Based Simulation Strategy. *Int. J. Geogr. Inf. Sci.* **2014**, *28*, 234–255. [CrossRef]
29. Zhang, Y.; Liao, X.Y.; Sun, D.Q. A Coupled InVEST-PLUS Model for the Spatiotemporal Evolution of Ecosystem Carbon Storage and Multi-Scenario Prediction Analysis. *Land* **2024**, *13*, 509.
30. Wu, Q.; Wang, L.; Wang, T.Y.; Ruan, Z.Y.; Du, P. Spatial–Temporal Evolution Analysis of Multi-Scenario Land Use and Carbon Storage Based on PLUS-InVEST Model: A Case Study in Dalian, China. *Ecol. Indic.* **2024**, *166*, 112448. [CrossRef]
31. Wei, Y.D.; Li, H.; Yue, W.Z. Urban Land Expansion and Regional Inequality in Transitional China. *Landsc. Urban Plan.* **2017**, *163*, 17–31. [CrossRef]
32. Tian, Y.Q.; Ouyang, H.; Xu, X.L.; Song, M.H.; Zhou, C.P. Distribution Characteristics of Soil Organic Carbon Storage and Density on the Qinghai-Tibet Plateau. *Acta Pedol. Sin.* **2008**, *45*, 933–942. (In Chinese)
33. Cheng, T.R. Research on the Forest Biomass and Carbon Storage in Xiaolong Mountains, Gansu Province. Ph.D. Thesis, Beijing Forestry University, Beijing, China, 1 April 2007.
34. Jia, G.M.; Liu, B.R.; Wang, G.; Zhang, B.L. The Microbial Biomass and Activity in Soil with Shrub (*Caragana korshinskii* K.) Plantation in the Semi-Arid Loess Plateau in China. *Eur. J. Soil Biol.* **2010**, *46*, 6–10. [CrossRef]
35. Lei, L.; Liu, X.D.; Wang, S.L.; Li, Y.; Zhang, X.L. Assignment Rule of Alpine Shrubs Biomass and Its Relationships to Environmental Factors in Qilian Mountains. *Ecol. Environ. Sci.* **2011**, *20*, 1602–1607.
36. Wang, C.T. Relationship between Productivity and Species Diversity of Plant Community in Alpine Meadow. Ph.D. Thesis, Northwest Institute of Plateau Biology, Chinese Academy of Sciences, Qinghai, China, 2006. (In Chinese).
37. Wang, X.X.; Dong, S.K.; Yang, B.; Li, Y.Y.; Su, X.K. The Effects of Grassland Degradation on Plant Diversity, Primary Productivity, and Soil Fertility in the Alpine Region of Asia's Headwaters. *Environ. Monit. Assess.* **2014**, *186*, 6903–6917. [CrossRef] [PubMed]
38. Geng, Y.; Wang, Y.H.; Yang, K.; Wang, S.P.; Zeng, H.; Baumann, F.; Kuehn, P.; Scholten, T.; He, J.S. Soil Respiration in Tibetan Alpine Grasslands: Belowground Biomass and Soil Moisture, but Not Soil Temperature, Best Explain the Large-Scale Patterns. *PLoS ONE* **2012**, *7*, e34968. [CrossRef] [PubMed]
39. Li, Y.Y.; Dong, S.K.; Wen, L.; Wang, X.X.; Wu, Y. The Effects of Fencing on Carbon Stocks in the Degraded Alpine Grasslands of the Qinghai-Tibetan Plateau. *J. Environ. Manag.* **2013**, *128*, 393–399. [CrossRef]

40. Yang, Y.H.; Fang, J.Y.; Ma, W.H.; Smith, P.; Mohammat, A.; Wang, S.P.; Wang, W. Soil Carbon Stock and Its Changes in Northern China's Grasslands from 1980s to 2000s. *Glob. Chang. Biol.* **2010**, *16*, 3036–3047. [CrossRef]
41. Ma, Y.J.; Zhong, J.T.; Mi, W.B.; Shi, J.L.; Jiang, X. Assessment and Vulnerability Analysis on Carbon Storage Based on Multi-Scenarios Simulation and Prediction of Land Use in Qinghai Lake Basin. *J. Arid Land Resour. Environ.* **2023**, *37*, 46–55. (In Chinese)
42. Hirota, M.; Kawada, K.; Hu, Q.W.; Kato, T.; Tang, Y.H.; Mo, W.H.; Cao, G.M.; Mariko, S. Net Primary Productivity and Spatial Distribution of Vegetation in an Alpine Wetland, Qinghai-Tibetan Plateau. *Limnology* **2007**, *8*, 161–170. [CrossRef]
43. Wu, Y.X.; Liu, F.N.; Chen, B.T. Spatial and Temporal Evolution and Drivers of Habitat Quality of Urban Agglomeration in Lower Yellow River Basin. *Bull. Soil Water Conserv.* **2023**, *43*, 396–404. (In Chinese)
44. Li, S.F.; Hong, Z.L.; Xue, X.P.; Zheng, X.F.; Du, S.S.; Liu, X.F. Evolution Characteristics and Multi-Scenario Prediction of Habitat Quality in Yulin City Based on PLUS and InVEST Models. *Sci. Rep.* **2024**, *14*, 11852.
45. Hou, Y.J.; Wu, J.M. Land-Use and Habitat Quality Prediction in the Fen River Basin Based on PLUS and InVEST Models. *Front. Environ. Sci.* **2024**, *12*, 1386549.
46. Liu, M.Z.; Zhang, H.J.; Wang, Y.F.; Pei, H.W. Characteristics of Habitat Quality in the Agro-pastoral Ecotone of Northern China Based on Land Uses. *Res. Soil Water Conserv.* **2021**, *28*, 156–162. (In Chinese)
47. Budyko, M.I. *Climate and Life*; Academic Press: New York, NY, USA, 1974.
48. Wu, L.; Luo, Y.K.; Pang, S.J.; Wang, G.S.; Ma, X.Y. Factor Analysis of Hydrologic Services in Water-Controlled Grassland Ecosystems by InVEST Model and Geodetector. *Environ. Sci. Pollut. Res.* **2024**, *31*, 20409–20433. [CrossRef] [PubMed]
49. Dri, G.F.; Fontana, C.S.; Dambros, C.S. Estimating the Impacts of Habitat Loss Induced by Urbanization on Bird Local Extinctions. *Biol. Conserv.* **2021**, *256*, 109064. [CrossRef]
50. Li, G. "Red Line of Ecological Protection": Lifeline to Ensure National Ecological Security. *Qiushi* **2014**, *2*, 44–46. (In Chinese)
51. *GB/T 30600-2022*; Well-Facilitated Farmland Construction—General Rule. Standardization Administration of China: Beijing, China, 2022.
52. General rules for high-standard cropland construction. *Agric. Compr. Dev. China* **2022**, *6*, 4–10. (In Chinese)